

# MEASURING THE TEMPERATURE OF A FLAME PROPAGATING THROUGH A QUARTZ TUBE USING HIGH SPEED COLOUR IMAGING AND THIN SiC FILAMENT BASED TWO COLOUR METHOD

Ma.Z.\*, Ebieto C. E., Zhang Y., and Woolley R.

\*Author for correspondence

Department of Mechanical Engineering,  
University of Sheffield,  
Sheffield, S1 3JD,  
United Kingdom,  
E-mail: [zma1@sheffield.ac.uk](mailto:zma1@sheffield.ac.uk)

## ABSTRACT

Blackbody radiation from a thin filament of SiC can be applied to measure hot gases temperature. The technique, Thin-Filament Pyrometer (TFP), exhibits fast temporal response and high spatial resolution owing to the very fine diameter and low heat conductivity. The advantage of this approach is the low cost and simplicity, and it is applicable to the situations where other approaches are difficult to apply. In this study, the investigation of methane-air flame propagating through a tube of a 20mm internal diameter quartz tube with open ends has been carried out. SiC fibres were installed at both ends and the midsection of the tube as radiation emitters. The required volume of methane at each equivalence ratio was measured and injected into the rig and the mixture was ignited at one end (left). The propagating flame was recorded using two high-speed cameras at a frame rate of 2000 fps with one tracking the speed of the flame and another capturing the images of the glowing filament. The images of the glowing filament were then processed to determine the surrounding gas temperature using the two-colour technique. Unlike the two-colour technique using beam splitting and narrow bandpass filtering approach, which often results in misalignment between two grey level images, complicated configuration and high cost, the current technique uses the camera built-in colour-banded filter. The ratio between two of the RGB primary channels was used for the calculation of the temperature. The maximum speed and temperature were observed at equivalence ratio 1.1 with a bell-shaped curve. For cases where the flames were subjected to instabilities, the temperatures were found to fluctuate accordingly. The accuracy of TFP measurement was verified by a commercial Infra-pyrometer.

## INTRODUCTION

Temperature is among the most frequently measured properties in combustion study. A temperature measurement technique having less-intrusive, fast-responding features, and being easily set-up, is desirable. A thin filament pyrometer is one of the candidates that matches several of the above characteristics, especially for high-temperature measurement in a closed space. This technique has been proven to be a useful approach to measuring flame temperature. It provides a one-dimensional profile of temperature measurement along the length of the filament.

## NOMENCLATURE

$C_2$	[-]	Second Planck's constant
$G(\lambda, T)$	[-]	Grey-level of Image
$k$	[W/mK]	Thermal Conductivity
$h$	[W/m <sup>2</sup> K]	Heat Transfer Coefficient
$Re$	[-]	Reynolds Number
$Nu$	[-]	Nusselt Number
$T$	[m]	True Temperature
$S$	[-]	Instrument Factor of Imaging System
$\lambda_R$	[m]	Wavelength in R Channel of the Imaging System
$\lambda_G$	[m]	Wavelength in G Channel of the Imaging System
$D$	[m]	Diameter of SiC Fibre.
$Pr$	[-]	Prandtl Number
$\varepsilon$		SiC fibre Emissivity
$T$	[K]	Surface Temperature

### Subscripts

$g$	Surrounding gas of the SiC fibre
$f$	SiC fibre
$G$	Green channel of the imaging system
$R$	Red channel of the imaging system
<i>Green</i>	Green channel of the imaging system
$a$	Ambient environment

Typically, TFP uses a  $\beta$ -SiC fibre of 15 $\mu$ m in diameter. It has good strength, relatively constant emissivity in the visible-wavelength band [1], resistance to oxidation with no catalytic effect, and a high melting point (3325K).

For temperature measurement, the fibre is placed in a thermal environment and the fibre glows and emits nearly black body radiation, which is detected by an imaging system, and the determination of the fibre temperature is based on the two-colour method. Finally, this temperature is correlated to the local gas temperature through an energy balance on the fibre.

Vilimpoc[2] pioneered the demonstration of the potential of measuring temperature using TFP and estimated the temporal response to be around 1.5ms. Bedat[3] applied the TFP measurement in a weakly turbulent flame and extended the limit of temperature to 550 K. Pitts[4] performed the TFP in flickering laminar diffusion flame. Struk[5] compared the temperature measured by thermocouple with the temperature measured by TFP within 3.5% difference for temperatures above 1200 K. Maun[6] applied a digital colour imaging based TFP measurement with an estimated uncertainty of  $\pm 60$ K in the range of 1400-2200K. Kuhn[7] compared the thin-filament-

derived gas temperature with the computational result, showing strong similarity. Bin[8] compared a laser-based technique and thermocouple with TFP measurement, showing good agreement in measured temperatures.

For all TFP measurements, energy balance is an important step to determine the surrounding gas temperature. The deviation between surrounding gas temperature and TFP determined temperature depends much on the accuracy of the energy balance procedure. SiC fibre is typically considered as a stable emitter and fibre temperature is determined from the incandescence of the glowing fibre by using two-colour method. This technique needs pre-calibration on a known temperature source, typically a tungsten lamp. Once this is done, it is free of further temperature calibration. In this paper, TFP is applied to measure propagating flame temperature in an open end tube. The variation of temperature and the hot gas velocity through the tube can be observed. The accuracy of two-colour method has been compared with an Infra-pyrometer. The main originality here is to explore the possibility of measuring fast developing hot gas by taking advantage of the good thermal properties of thin SiC fibre.

## EXPERIMENTAL SETUP

The experimental rig consisted of a tube with an inner diameter of 20 mm and a length of 1200 mm, opened at both ends. The central 700mm length of the tube was made of quartz to provide optical access (Fig. 1). The quartz was used because of its high transmissivity and the ability to survive in a high-temperature environment. SiC fibres were installed at the midsection and both ends of the quartz tube. The experiment was conducted at different equivalence ratios of 0.9, 1.0, 1.1 and 1.2. The required volume of methane at each equivalence ratio was measured and injected into the rig using a syringe, and two fans attached to the rig were used to create a homogeneous mixture. The propagating flame was recorded using two high-speed cameras at a frame rate of 2000 fps with one tracking the speed of the bluish flame and the other capturing the images of the only glowing filaments for flame temperature measurement using a higher shutter speed to eliminate the disturbance of the flame illumination and avoid image saturation as a result of the fibre strong emission. Ignition was initiated using a pilot flame. This was done by opening a port at the left end of the tube after switching off the fan and directing the pilot flame into the tube.

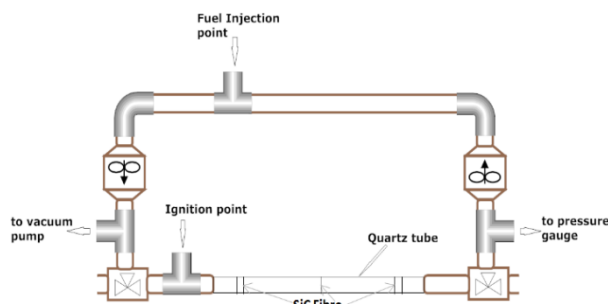


**Figure 1** Experimental setup for flame temperature measurement; there are two fibres at each end of the tube and one in the middle.

The gas phase temperature cannot be directly measured by the thin filament pyrometer. Instead, the surface temperature of the fibre is determined first, followed by an energy balance analysis to evaluate the temperature difference between the fibre and its surrounding gas. It involves solving the energy conservation equations on a fragment of the fibre. In this research, two-colour method was used to determine the fibre temperature; it will be discussed in the next section.

## THE METHOD OF TWO-COLOUR PYROMETER

Two-colour method has been widely used over the last decade, because of its ability to measure the surface temperature of grey body without knowing the emissivity. This principle can be found elsewhere [9-11]. In this study, the fibre temperature can be calculated by deriving the ratio of the colour-banded images captured by the high-speed colour digital camera, instead of utilising the narrow bandpass filtering and beam-splitting approach in order to avoid the complex configuration and optical attenuation. Each image captured by the RGB camera can be separated into three different channels corresponding to the red, green and blue sub-images in the visible wavelength band. For this research, we have used the R and G channel in the two colour technique for determining the fibre temperature because the radiation detected in the B channel was much weaker than that detected in the R and G channels (Eq. 1).

$$T = \frac{C_2 * (\frac{1}{\lambda_G} - \frac{1}{\lambda_R})}{\ln \frac{G(\lambda_R, T)}{G(\lambda_G, T)} + \ln \frac{S_{\lambda_G}}{S_{\lambda_R}} + \ln (\frac{\lambda_R}{\lambda_G})^5} \quad (1)$$

Where S ratio was determined through the calibration procedure using a pre-calibrated tungsten lamp ranging from 1225 to 2497 K; the RG Ratio responses of the imaging system in this range can be found in Fig.2

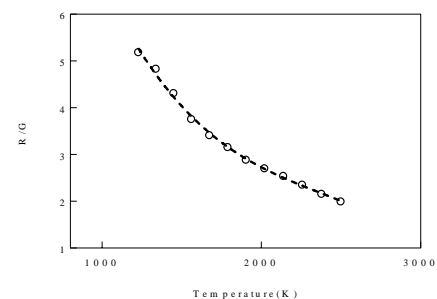


**Figure 2** Temperature calibration between the RG ratio and the true temperature

## Accuracy of the two-colour approach

Prior to measuring the flame temperature in the quartz tube, the fibre temperatures measured by the two-colour method and the Infra-pyrometer have been compared. This comparison test used a stable Methane/Air premixed flame on a Bunsen burner. Four fibres were placed in the flame at different heights and hung tautly on a U-shape frame. An IMPAC Infra-pyrometer was applied here to compare with the two-colour method; this pyrometer can offer single-spot temperature measurement with a declared accuracy of 1%, and only able to measure grey-body

temperature with known emissivity. The spot size is a function of the distance between the measured object and the Infra-pyrometer. Fig3 shows the measured area of each fibre marked by black circles. The time-dependent temperature variation of three single points has been measured by both the Infra- and two-colour pyrometer in 0.1 secs with a 0.01 secs interval. The comparison of measured temperatures is presented in Fig 4.



**Figure 3** The position of measured points on each glowing SiC fibre; each spot is equivalent to 4mm in length of fibre corresponding to 30 pixels in the image

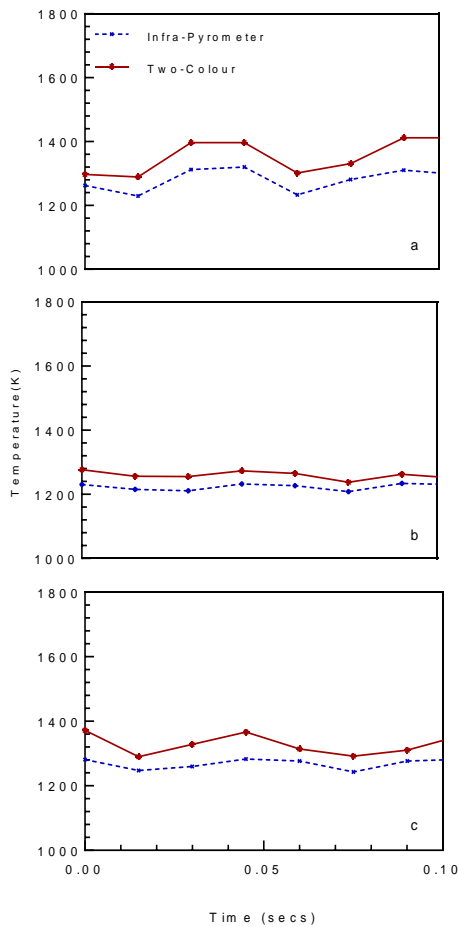


**Figure 1** Comparison of measured time-dependent temperatures by the two-colour and the Infra-pyrometer on

each SiC fibre. a, b and c present the compared measured temperatures at position P1, P2 and P3, respectively.

The two-colour method measured fibre temperatures are slightly higher than that measured by the Infra-pyrometer. The measured temperature differences between these two approaches are 6%, 2.7% and 4.7% at P1, P2 and P3 respectively.

### THERMAL BEHAVIOUR OF THE FILAMENT

The actual local gas temperature and the fibre temperature are different and are related by the steady-state energy balance equation (Eq. 2). It is a typical heat transfer problem as the fibre is heated by its surrounding hot gas and cooled by radiation loss. For the case of the thin filament, the conduction loss or gain in the axial direction is negligible because the ratio of the circumferential to cross-sectional area is large; thus, the heat transfer rate by radiation and convection is much higher than the axial conduction heat transfer. The gas temperature calculation can be obtained by

$$T_g = \frac{\varepsilon\sigma(T_f^4 - T_a^4)}{h} + T_f \quad (2)$$

It is obvious that the first term on the right-hand side represents the difference between the gas and the fibre temperature; the ambient temperature  $T_a$  refers to the quartz tube temperature which is assumed to be the room temperature. In order to determine this difference, the heat transfer coefficient must be determined. This coefficient can be determined using the equations below:

$$Re = \frac{\rho V D}{\mu} \quad (3)$$

$$Nu = (0.35 + 0.56 Re^{0.52}) Pr^{0.3} \quad (4)$$

$$h = \frac{Nu * k}{D_f} \quad (5)$$

Where the heat transfer coefficient comes from a Nusselt number correction for forced convection over a cylinder, this number is valid for  $10^{-1} < Re < 10^5$  [12]. The fluid properties must be determined by the average of gas and ambient temperatures. Because the gas temperature is unknown, an iterative method has to be applied for the temperature correction.

The algorithm utilised to estimate the heat loss is reviewed below. The fibre temperature determined by Eq.(1), is assumed to be the gas temperature. The mole fraction of major species concentration calculated via an adiabatic equilibrium chemical reaction at corresponding equivalence ratio in each case. Then the mole fraction based transport properties can be found and used to calculate the Reynolds number and the Nusselt number by the relationship in Eq.(3) and Eq.(4), respectively. Since the quantity required is the average heat transfer coefficient, the average flame velocity passing through the fibre was used to calculate the Reynolds number. Once the Reynolds Number is found, the average heat transfer rate can be computed and used to calculate the corrected  $T_g$  in Eq.(2). The entire process is repeated twice to obtain a more accurate corrected temperature.

## RESULTS AND DISCUSSIONS

In order to have a better understanding of the flame temperature variation to be presented later on, the behaviour of the flame propagation has to be clarified first.

High-speed imaging visualisation has shown that the flame developed with relatively weak oscillation at the left side of the tube, then, at the middle the flame oscillation was stronger; finally, the oscillation experienced a reduction towards the end of the tube. In Fig.5, the image shows the emission variation at the middle of the tube, captured by a mono-colour camera at 2000 frames per second (fps). It can be seen that the middle fibre emitted radiation at its centre first, then it gradually increased towards each end of the fibre. This implies that higher temperature is observed at the mid-section of the glowing fibre compared to those nearer the tube walls.

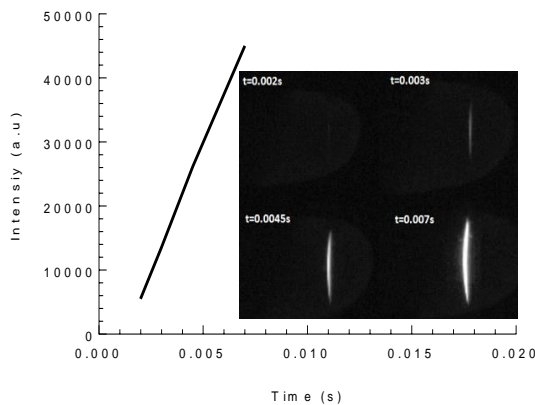


**Figure 2** The glowing fibre as the flame crossed through tube middle section and time-dependent pixel brightness intensity response

Fig. 6 illustrates the behaviour of the strong flame oscillation in the middle of the tube. It can be observed that the flame boundary layer changed from being irregular to a semi-circular shape for a complete cycle of oscillation; these oscillations continued and gradually dimmed towards the tube end; this finding may account for the pattern of the time-dependent temperature variation shown in Fig. 7

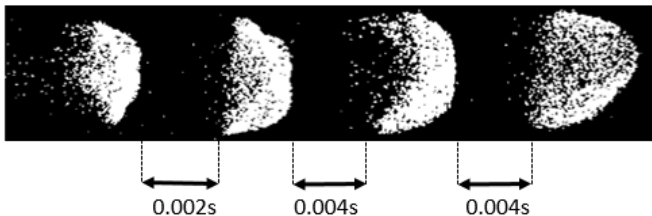


**Figure 3** The behaviour of flame oscillation inside the tube

With reference to the gas temperature measurement, the imaging system of TFP pyrometer separately captured each glowing fibre placed at the middle and each end of the tube. At each location, the gas temperature was measured at three

different equivalence ratio settings. It was not possible to image all fibres simultaneously because that would have caused a significant drop in spatial resolution. Fig.7 shows the locally derived gas temperature variation at the different fibre positions. Fig. 7b illustrates a stronger oscillation in gas temperature than that shown in Figs. 7a,c. Fig. 7a shows the gas temperature variation at the location near the ignition point, with two fibres placed 3mm apart. It depicts a similar variation of the gas temperature, which indicates a small thermal gradient between these two fibres. At the end of the tube Fig. 7c shows a moderate gas temperature variation. For all cases, obvious fibre deflection has not been observed; the flame temperature variations are mainly due to flame instabilities which are stronger at the middle of the tube.

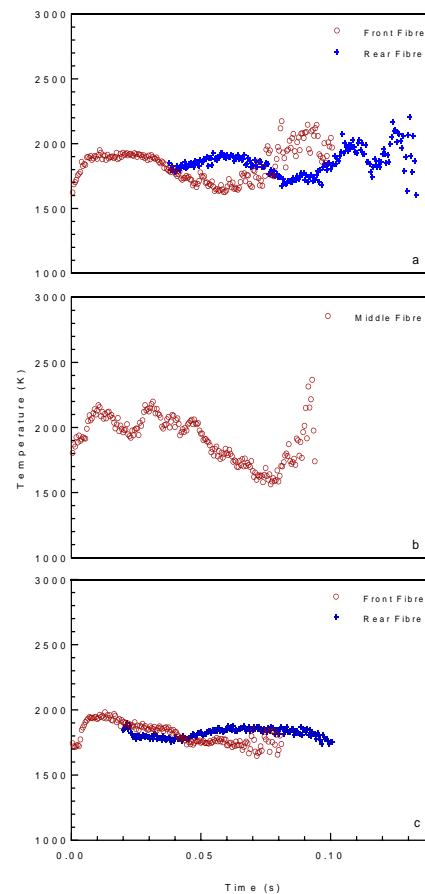


**Figure 4** Time-dependent gas temperature variation at equivalence ratio = 1.1. (a) Temperature variation at the left end of the tube near ignition place, (b) Temperature variation at the middle of the tube, (c) Temperature variation at the right end of the tube.

In addition, the time-dependent pressure oscillation of the flame travelling through the tube from the left to the right end of the tube was also recorded. As can be seen in Fig.8, the amplitude of oscillation was relatively moderate before 0.1s, afterwards, the peak amplitude occurred around 0.2s which correspond to the position of the middle section of the tube,

finally, the amplitude was gradually tailed off by the tube right end. This behaviour was similar to the time-varied variations of gas temperatures detected by the two-colour pyrometer.

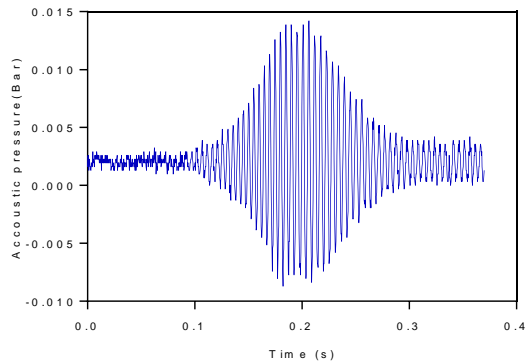


**Figure 5** The pressure readings inside the tube at equivalence ratio = 1.1.

Furthermore, by using the illumination from each fibre the variation of the flame oscillation could also be observed. The captured RGB images of each glowing fibre were converted to grey images, and then only brightness intensity of pixels within the glowing fibre was summed up as the total intensity. Fig. 9 a,b,c show the cycle of heating up and cooling down as the flame passed each fibre at similar cycling time. The cooling rate increased from left to right of the tube. Fig. 9 d,e,f show the plots of the flame amplitude against the frequency, with the highest flame frequency occurring at the middle section of the tube.

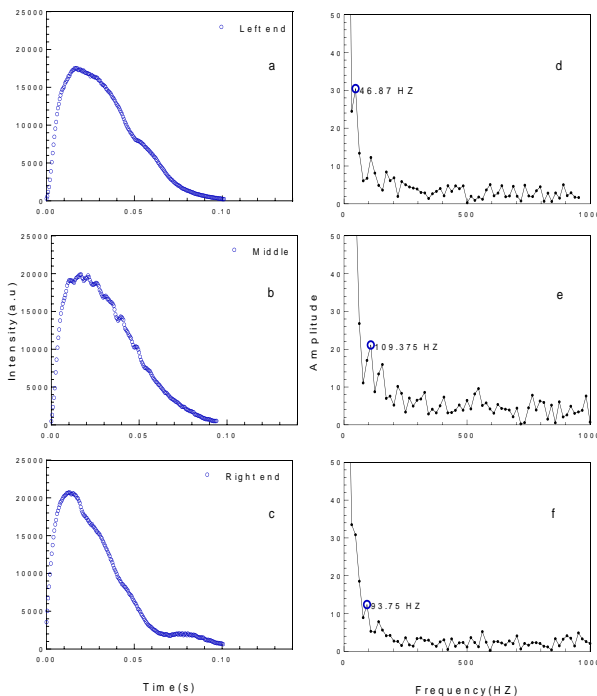


**Figure 6** a, b and c are experimental heat-up and cool-down

cycle at Left-end, Middle and Right end of the tube. d, e and d present the main frequency of intensity oscillation at the corresponding positions of the tube, using FFT.

The fibre and the corrected gas temperatures varying with equivalence ratio are shown in Fig. 10, where each point averages 162 samples. The common trend shows that the temperatures increased from  $\phi=0.9$ , peaked at  $\phi=1.1$ , and then decreases until  $\phi=1.2$ , which is similar to the flame velocity variations shown in Fig. 11 Both the highest flame velocity and gas temperature were found at  $\phi=1.1$ .

The difference between each gas-fibre temperature combination was evaluated as shown in Fig. 12. This difference is larger for flames at the middle section of the tube.

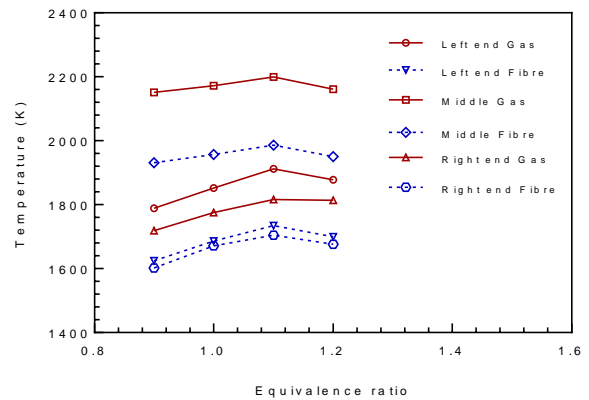


**Figure 70** The average temperature of flame travelling through the fibre at different equivalence ratios

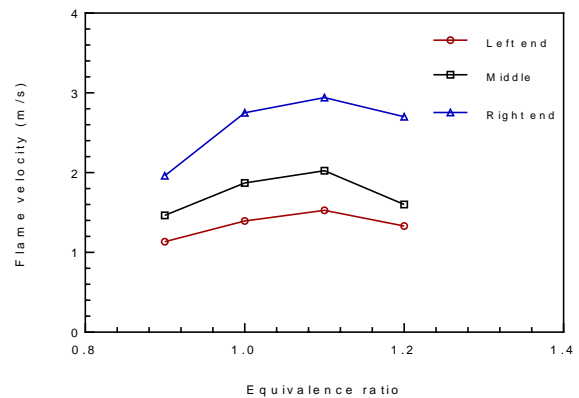


**Figure 8** Flame velocity varying with equivalence ratio

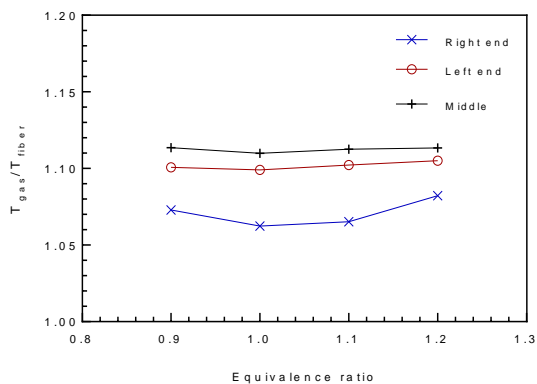


**Figure 9** The ratio of the gas and fibre temperature varying with equivalence ratio

Finally, the temperature correction between the fibre and its surrounding temperature is derived from the energy balance. This balance involves the convective heat transfer from the gas to the fibre, heat loss via radiation from the fibre to its ambient environment. The conductive heat transfer along the fibre is discounted because it has a limited effect in the heat transfer process. Since the gas temperature is not directly measured, it is important to consider the potential errors and their effect on the accuracy of the gas temperature measurement.

The main uncertainties in the measurement of the gas temperature are in the calculation of the fibre temperature, the emissivity of the fibre, and the convective heat transfer coefficient. Moreover, there are several sources of uncertainty in the determination of Nu number; firstly, the correlation may not fully fit to the flow conditions used in the experiment. Secondly, knowing the Reynolds number (Re) is required to calculate Nu number, which implies the knowing of the gas velocity perpendicular to the fibre. In this study, only the averaged velocity passing the fibre was estimated by the imaging-based techniques. Finally, the thermal properties of the gas are functions of temperature and gas composition, which are both estimated in the study.

Regarding the other variables, the tolerance of the fibre diameter and its emissivity depends on oxidation resistance and the roughness of the fibre which probably vary in the high-temperature environment. The obvious uncertainty exists in the determination of the fibre temperature. Fig. 2 shows the measured temperature difference between using the two-colour and the Infra pyrometers. This error could arise from the partial misalignment of the measured spot area using the two techniques, and the fibre emissivity may not be consistent along the length of the fibre.

## CONCLUSION

In the present work, we compared single point fibre measurement using the TFP- and the commercial Infra-pyrometer. Measured temperatures by the two pyrometers were found to be in good agreement with acceptable difference in temperature. The calibrated TFP was then applied to measure the temperature of a flame propagating through a 20mm diameter quartz tube by installing SiC fibres at different positions of the tube. Both the time-dependent gas temperature and the pressure oscillations reached their peaks at the middle section of the tube. The gas temperatures found at the mid-section of the glowing fibre were higher than that nearer the tube walls. Finally, the major sources of uncertainty in gas temperature have been discussed. Based on our results, it has been shown that the TFP approach has the potential to track the temperature variation of fast moving hot gases. Hence, it could be a promising tool for fast temperature measurement.

## REFERENCES

- [1] D. Alfano, *Spectroscopic properties of carbon fibre reinforced silicon carbide composites for aerospace applications* 2011.
- [2] V. V. a. L.P.Goss. (1988). *SiC-based thin-filament pyrometry: theory and the thermal properties*.
- [3] T. f. i. p. i. t. profile and m. i. a. w. t. h. p. flame, "<SiC Bedat.pdf>."
- [4] W. M.pitts, "Temperature Uncertainties for Bare\_bead and Aspirated Thermocouple Measurements in fire Environment," *The Foundation of Fire Standards*.
- [5] W. M.PITTS, "Thin-filament pyrometry in flickering laminar diffusion flames," presented at the Twenty-Sixth Symposium on Combustion, 1996.
- [6] P. B. S. Jinesh D.Maun, and David L.Urban, "<Thin-filament pyrometry with a digital still camera.pdf>," *APPLIED OPTICS*, vol. 4, pp. 483-488, 2007.
- [7] P. B. Kuhn, B. Ma, B. C. Connelly, M. D. Smooke, and M. B. Long, "Soot and thin-filament pyrometry using a color digital camera," *Proceedings of the Combustion Institute*, vol. 33, pp. 743-750, 2011.
- [8] B. Ma, G. Wang, G. Magnotti, R. S. Barlow, and M. B. Long, "Intensity-ratio and color-ratio thin-filament pyrometry: Uncertainties and accuracy," *Combustion and Flame*, vol. 161, pp. 908-916, 2014.
- [9] D. Sun, G. Lu, H. Zhou, and Y. Yan, "Flame stability monitoring and characterization through digital imaging and spectral analysis," *Measurement Science and Technology*, vol. 22, p. 114007, 2011.
- [10] Z. Ma and Y. Zhang, "High temperature measurement using very high shutter speed to avoid image saturation," pp. 246-253, 2014.
- [11] Y. H. a. Y.Yan, "Transient two-dimensional temperature measurement of open flames by dual\_spectral image analysis," *SAGE*, vol. 22, pp. 371-384, 2000.
- [12] J. P. Holman, *Heat Transfer*. New York: McGraw, 2008.